DOI 10.1007/s10891-016-1356-1

Journal of Engineering Physics and Thermophysics, Vol. 89, No. 1, January, 2016

EXPERIMENTAL STUDY OF THE EFFECTS OF COLLISION OF WATER DROPLETS IN A FLOW OF HIGH-TEMPERATURE GASES

D. V. Antonov, R. S. Volkov, G. V. Kuznetsov, and P. A. Strizhak

UDC 536.4

Using high-speed video recording and cross-correlation "tracer" visualization, the authors have investigated the regularities of the processes of collision of water droplets (characteristic parameters: radii 0.025–0.25 mm, velocities of motion 0.5–12 m/s, and relative concentration 0.001–0.0012 m^3 of liquid droplets in 1 m^3 of the gas) in their motion in a flow of high-temperature (about 1100 K) gases. The characteristic effects of collision of two droplets, at which combined droplets are formed (coagulation occurs) and conditions for spreading or fragmentation of the latter are implemented, have been singled out. The values of the Weber and Reynolds numbers for droplets before and after the collisions have been established. The influences of the velocities of motion, the dimensions, and the angles of intersection of mechanical trajectories of droplets on the effects of collisions have been determined.

Keywords: *droplets of a liquid, droplet flow, collision, fragmentation, spreading, high-temperature gases, high-speed video recording.*

Introduction. Fire-suppression systems (sprinklers) using finely atomized water, "water mist," and "water curtains" [1–8], which have received wide recognition in recent years, are based on feeding finely divided droplet water flows to the flame zone. As a result of theoretical [9–12] and experimental [13–18] investigations, we have established minimum dimensions and the number of droplets of extinguishing liquids based on water emulsions, and also distances between these droplets sufficient for active absorption of the fire energy. Important features illustrating the high probability of coagulation of droplets of a sprayed liquid in a gas medium have been singled out in the experiments of [16–18]. This process makes it much more difficult to select minimum droplet dimensions sufficient for use in the considered applications. Also, conditions under which, upon the collision of two droplets, the latter are crushed rather than coagulate have been singled out in analyzing videograms of the experiments of [16–18]. Due to the vaporization and difficulties with determining the "liquid–gas" interface accurately, these features could only be recorded using panoramic optical methods of "tracer" visualization (in particular, PIV (Particle Image Velocimetry) [19–21] and IPI (Interferometric Particle Imaging) [22–24]), the cross-correlation system, and high-speed (up to 10^5 frames per second) video-recording facilities. It is of interest to analyze the regularities of collision of two droplets in the flow of high-temperature gases using the separated software and hardware system. Here, it is important to limit the range of the initial dimensions (d_0) and velocities of motion (u_0) of droplets not only in accordance with the capabilities of today′s sprayers (e.g., [1–8]) but also by ensuring conditions for preservation of the monolithic character of the droplets (absence of their fragmentation before the collision with neighboring ones). The experiments of [25–30] have made it possible to establish that, for many liquids (in particular, water) in common use and for their suspensions, conditions for fragmentation of droplets in a gas medium are characterized by an excess over the limiting values of the Weber number (We) of 7 to 10 (depending on the basic properties of the liquid). Therefore, when the regularities of droplet collision are analyzed (particularly under the conditions of intense phase transformations), one should ensure the observance of the conditions We < 7 for each of the investigated droplets of the flow.

The present work seeks to statistically analyze the effects of collision of two water droplets on a flow of high-temperature gases under the conditions of intense phase transformations using panoramic optical methods of "tracer" visualization.

Experimental Bench and Procedure of Investigations. In the course of the investigations, we used an experimental bench (Fig. 1) analogous to those used in the experiments of [13–18] as far as the basic elements are concerned. Unlike in

National Research Tomsk Polytechnic University, Institute of Power Engineering, 30 Lenin Ave., Tomsk 634050, Russia; email: romanvolkov@tpu.ru. Translated from Inzhenerno-Fizicheskii Zhurnal, Vol. 89, No. 1, pp. 94–103, January–February, 2016. Original article submitted February 4, 2015.

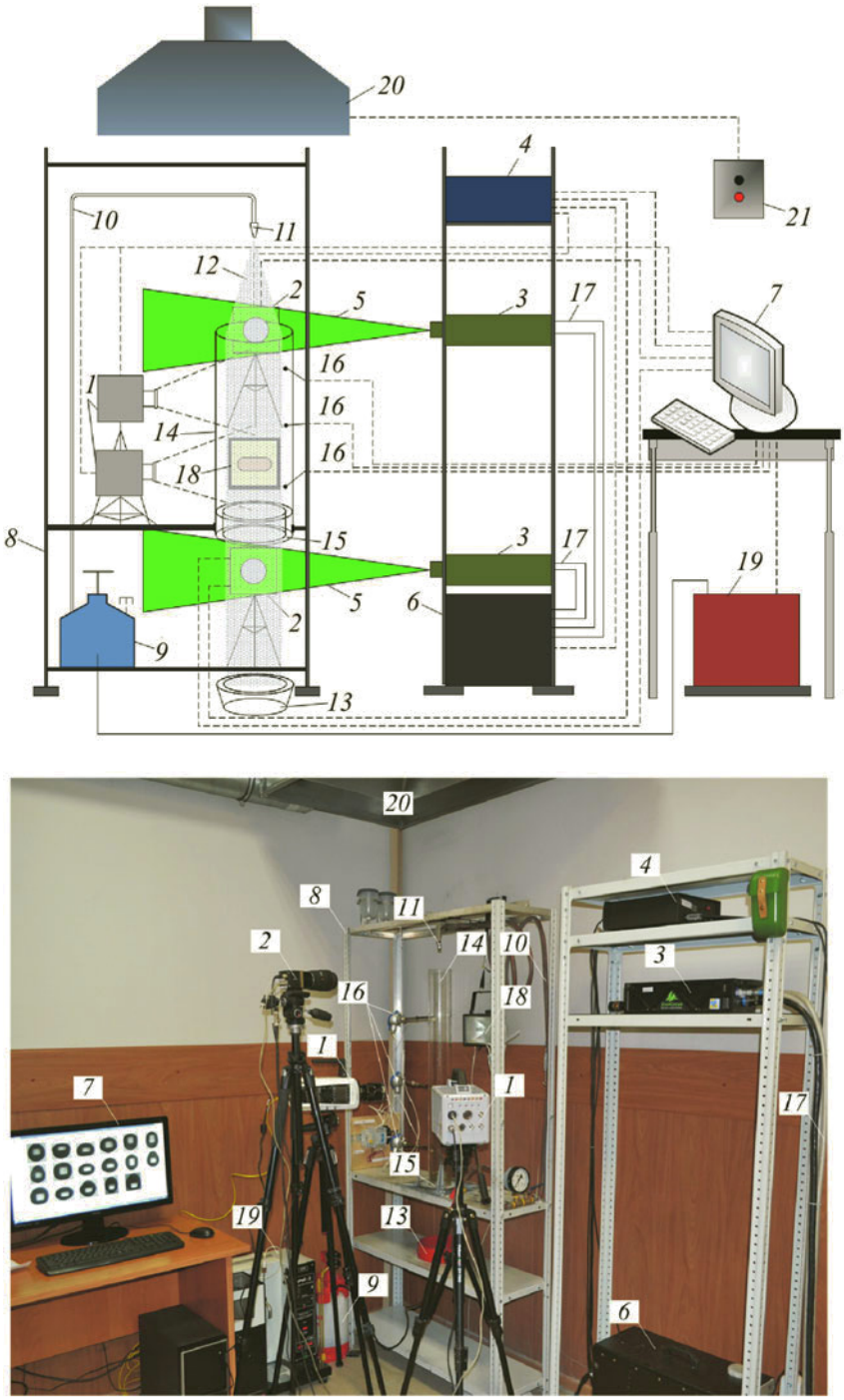

Fig. 1. Diagram (a) and the appearance (b) of the experimental setup: 1) high-speed video camera; 2) cross-correlation camera; 3) double solid-state pulsed laser; 4) synchronizer of the personal computer, the cross-correlation camera, and the laser; 5) light "knife;" 6) laser-radiation generator; 7) personal computer; 8) stand; 9) water-filled vessel; 10) channel for feeding water (water duct); 11) sprayer; 12) sprayed water; 13) catcher; 14) cylinder manufactured from heat-resistant transparent material; 15) hollow cylinder into whose internal space a fuel liquid is poured; 16) thermocouples; 17) channel of motion of the laser′s cooling liquid (coolant duct); 18) floodlight; 19) heating unit; 20) injection system; 21) on/off control panel of the injection system.

[13–18], two high-speed (up to 10^5 frames per second) video cameras were used in addition to the cross-correlation video system. The software system used to process videograms obtained during the investigations incorporated "Tema Automotive" and "FastCam." The software used allowed an instantaneous analysis of the coordinates of the position and the shape of droplets, and also of their velocities, accelerations, angles, covered distances, and other parameters with their variation in a wide range. The cited system enabled us to record the dynamics of variation in the parameters of all the droplets brought into the recording region.

Analogously to the experiments in [13–18], we recorded images of water droplets in the process of their motion through the products of combustion of kerosene in a hollow cylinder (height 1 m, inside and outside diameters 0.2 and 0.206 m) manufactured from heat-resistant transparent glass. Video recording was performed throughout the length of the cylindrical channel. As a result of the processing of videograms, we selected more than 500 frames with characteristic collisions of the droplets at different dimensions, velocities of motion, and angles of interaction of mechanical trajectories of the latter.

The initial droplet dimensions (radii) in the flow of a sprayed liquid ranged from 0.025 to 0.25 mm. The relative volume concentration of the droplets γ_m was maintained in the range 0.001–0.0012 m^3 of liquid droplets in 1 m^3 of the gas. Selection of the ranges of variation in γ_m and in the concentration of the droplets in the flow γ_m is determined by specific limitations of panoramic optical "tracer"-visualization methods PIV [19–21] and IPI [22–24] employed in processing experimental videograms.

The velocity of motion of the combustion products u_g was controlled using injection system 20 and was about 1.5 m/s in all the experiments (analogously to the experiments in [13–18]). The velocities of motion of the droplets in the flow of high-temperature gases u_m ranged from 0.5 to 12 m/s (the range corresponds to a large number of applications, e.g., [1–8]).

To measure the velocity of motion of the water droplets u_m and the gases u_g we employed the PIV panoramic optical method [19–21]. The velocities of travel of the gases (combustion products) in channel 14 were determined before the injection of droplets of the sprayed liquid. "Tracing" particles (titanium dioxide was used) were introduced into the gas flow in the lower part of the channel 14. Analogously to the procedures of [15–18], we recorded instantaneous distributions of the "tracer" velocities in the gas flow between laser flashes.

An algorithm for finding the instantaneous velocity distributions by means of the PIV method is based on determining distances covered by the "tracers" during a fixed time interval between laser flashes. Here, cross-correlation camera 2 records a couple of frames. Each of the taken videograms is subdivided into elementary computational domains in accordance of the algorithms [19–21]. Next, using Fourier transformations, we find the maximum of a correlation function which determines the travel of the "tracers." Thereafter, using the scale factor (determined in the initial stage of the experiments at the instant of calibration of the optical system) and a known time delay, we recalculated the velocity in m/s.

The droplet dimensions were determined with the IPI method [22–24]. The procedure of computations of droplet dimensions by the IPI method is based on the difference in refractory indices of the air and aqueous media. When the dimensions are determined, images of the droplets are photorecorded by a pre-calibrated cross-correlation camera 2 defocused in a special manner (using a special aperture). The droplets are illuminated by laser "knife" 5. This results in the images of droplets on the videograms. These images are narrow bands with a set of interference fringes representing the light reflected and singly refracted by the droplets. Next, according to the number of interference fringes, the dimension of each droplet in the recording region is computed using special algorithms [22–24]. This makes it possible to obtain an instantaneous distribution of the dimensions of water droplets.

Algorithms for determining the velocities of motion and the dimensions of droplets after their coagulation are analogous to those presented above.

The systematic errors in determining the dimensions r_m and the velocities u_g and u_m using PIV and IPI panoramic optical methods, and also the corresponding video-recording experimental bench, were no larger than 1.6 and 2.1%. The maximum random errors in determining the parameters in question amounted to 2.1% for r_m and to 3.4% for u_g and u_m.

Also, in processing experimental videograms, we determined the angles of intersection of mechanical trajectories of droplets at the instant of their collision α_m using "Tema Automotive" specialized software and a parametric net on the videograms.

Investigations were carried out for a kerosene flame with a gas temperature T_g of about 1100 K in the cylinder channel 14. Measurements were performed by three Chromel–Alumel (range of the measured temperatures 273–1373 K and systematic error ±3 K) thermocouples installed at different heights (0.15 m, 0.5 m, and 0.85 m) in the cylinder 14. The

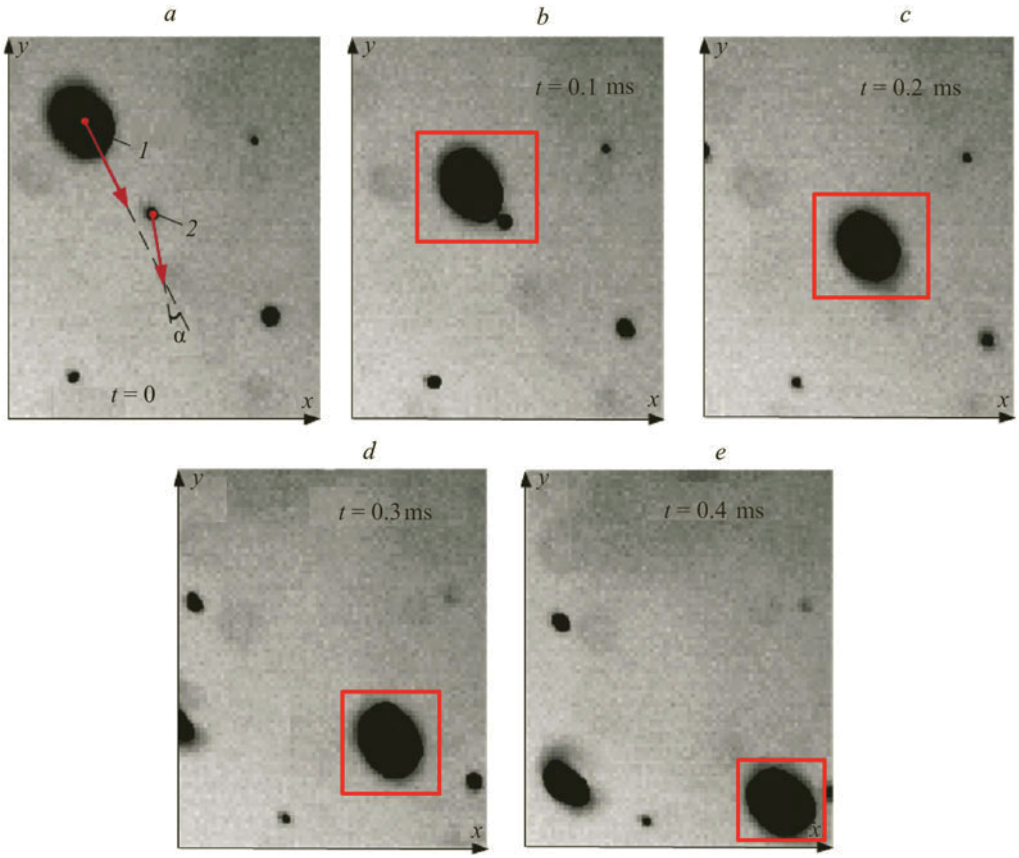

Fig. 2. Typical videograms with the coagulation of droplets upon collision.

initial temperature of water droplets introduced into the gas medium T_w was held at about 300 K using a system of heating chambers and a Chromel–Copel thermocouple (range of the measured temperatures 273–473 K and systematic error ±1.5K). The maximum random error in measuring T_g were as large as 20 K. For T_w, this parameter did not exceed 3 K.

To assess measurement errors in the conducted experiment, we used the procedures from [31–33].

Results and Discussion. The conducted experiments have shown that there can be three variants of effects (results) of collisions for the processes of interaction of two droplets of sprayed water in the flame zone. When the first variant is implemented, the droplets coagulate (Fig. 2), and a combined droplet continues to move in the flow until the next collision occurs. The second variant: after the collision there form two droplets with similar pre-collisional dimensions (Fig. 3). Such interaction of droplets may be considered to be their spreading. The third variant is characterized by the fragmentation of two colliding droplets into a group (no less than five droplets in it) with substantially smaller dimensions than the initial ones (Fig. 4).

An analysis of the videograms of the conducted experiments with the revealed results of droplet collisions has shown that each of the three variants of collisions is implemented quite frequently. However, the frequency of their implementation changes significantly with travel velocities, dimensions, and angles of intersection of mechanical trajectories of droplets in the flow of high-temperature gases.

Figure 5 gives typical videograms with the images of droplets of sprayed water in the high-temperature flow, the characteristic "tracer" velocities, and typical mechanical trajectories of the droplets. From an analysis of Fig. 5, we can draw the conclusion on the substantial nonmonotony of velocity curves and on the complex mechanical trajectories of the droplets. This in turn explains the probabilistic character of collision of the latter. As a consequence, it is expedient to use statistical approaches to explain the revealed regularities of collisions.

From the results of processing of experimental data, we have determined the frequencies of implementation of each of the three established variants of effects of collisions (Fig. 6) as functions of the velocities of colliding droplets and their

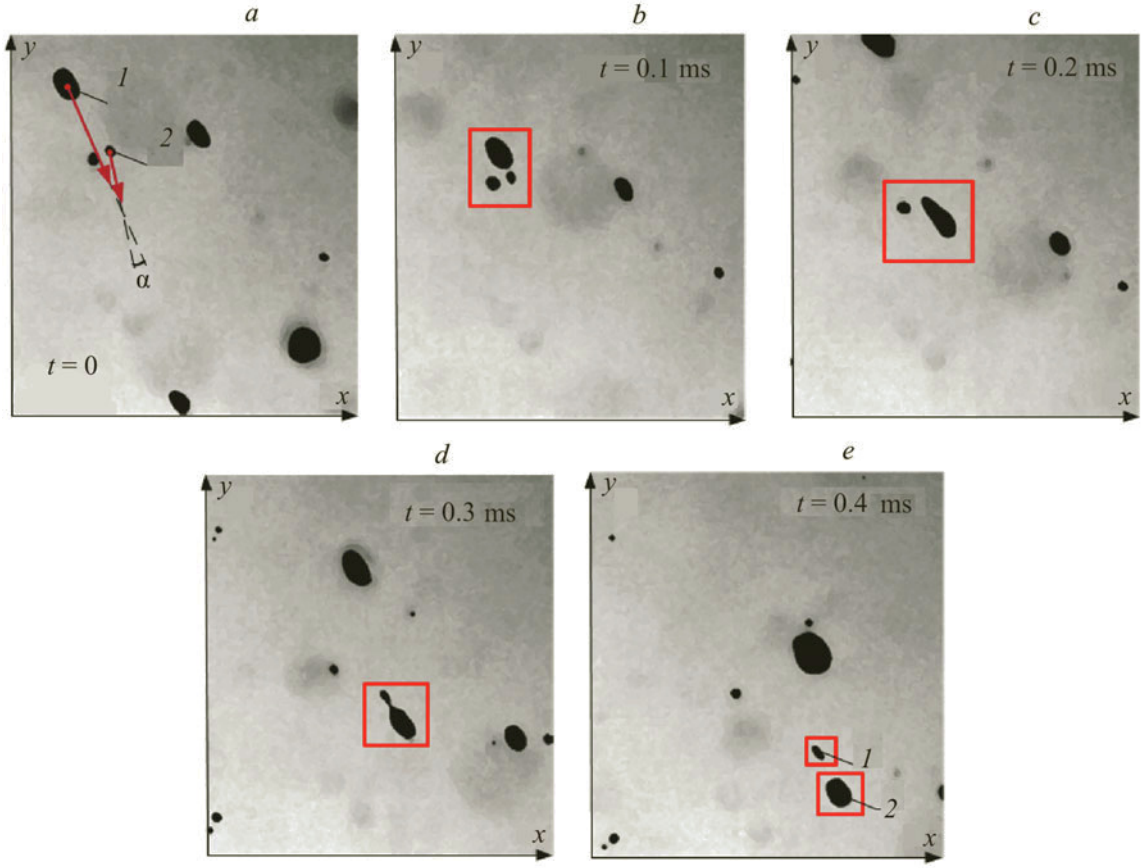

Fig. 3. Typical videograms with the spreading of droplets upon collision.

dimensions. Also, Fig. 6 gives maximum and minimum values of generalizing dimensionless numbers, i.e., Reynolds and Weber numbers of colliding particles:

$$\mathrm{Re}_{m1} = \frac{2u_{m1}r_{m1}}{\nu}, \quad \mathrm{Re}_{m2} = \frac{2u_{m2}r_{m2}}{\nu},$$

$$\mathrm{We}_{m1} = \frac{2u_{m1}^2 r_{m1}\rho_g}{\sigma}, \quad \mathrm{We}_{m2} = \frac{2u_{m2}^2 r_{m2}\rho_g}{\sigma},$$

where ν is the kinematic viscosity of the gas maximum, m^2/s, ρ is the gas density, kg/m^3, and σ is the surface tension of the liquid, N/m.

In computing the Reynolds and Weber numbers, we disregarded the characteristic velocities of motion of the gases in the channel under study due to the small values of u_g compared to the velocities of motion of the droplets.

Figure 7 gives the frequencies of implementation of the established collision regimes with variation of u_{m1} from 20 to 10 m/s and change in u_{m2} in the range 2–3 m/s. It is quite easily seen (Fig. 7) that, at small and comparable velocities of motion of water droplets, the coagulation frequency is maximum. Here, the values of the frequencies of spreading and fragmentation of the droplets are minimum. With growth in the difference in velocities of motion of colliding droplets, the characteristic coagulation frequencies decrease considerably. This decrease is accompanied by the growth in the corresponding frequencies of spreading and fragmentation. At a difference in velocities of travel of colliding droplets, which is maximum for the conducted experiments, the frequencies of all the three variants are comparable and are from 0.25 to 0.45.

Also, it has been established that a growth in the difference of the characteristic dimensions of the droplets tends to increase the frequency of their fragmentation (Fig. 7). The obtained results are attributable to the fact that when the velocities and dimensions of the droplets are comparable, their momenta are similar. As a consequence, the viscosity and surface-

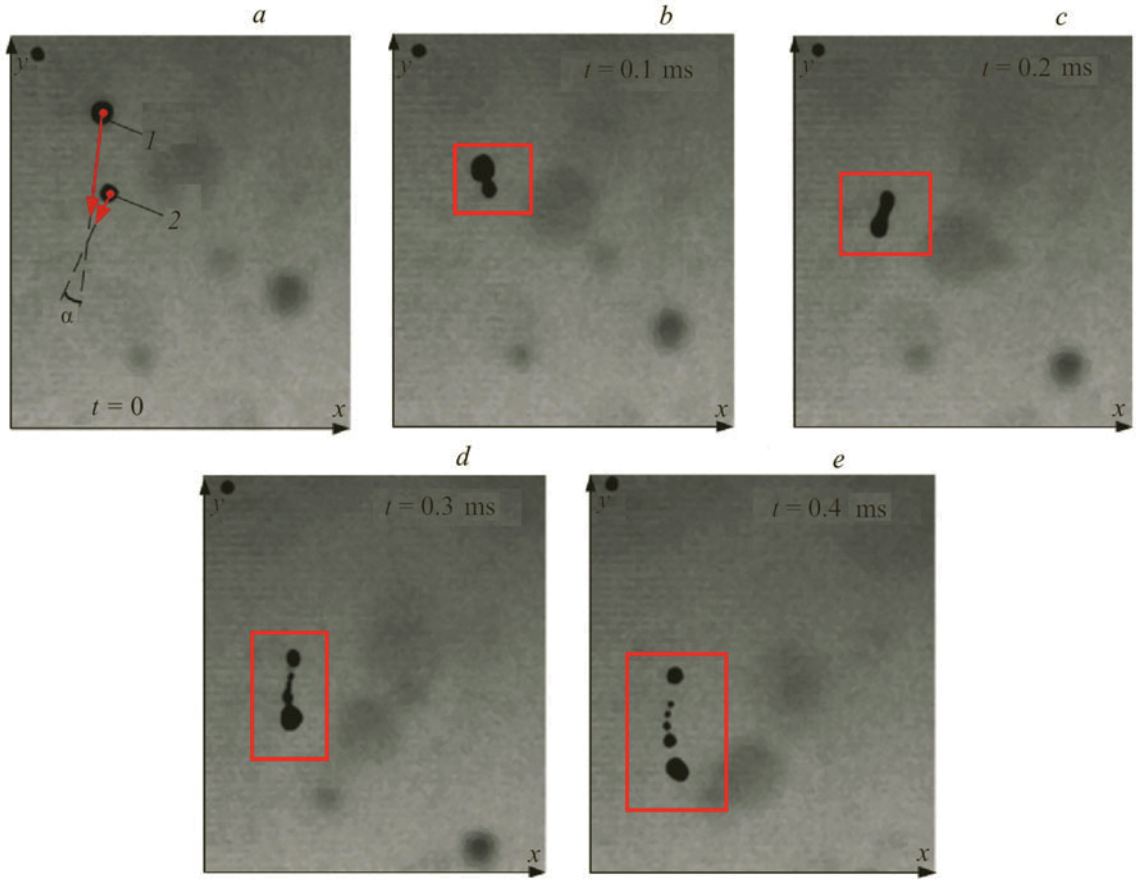

Fig. 4. Typical videograms with the fragmentation of droplets upon collision.

tension forces exceed the inertial forces as they collide, and the coagulation frequencies are maximum. With growth in the difference of the velocities or dimensions of colliding droplets, the momenta differ. Inertial forces grow in relation to the forces of viscosity and surface tension. As a consequence, the frequencies of spreading or fragmentation of the droplet grow.

An analysis of the results of collisions makes it possible to infer that, as the difference of the dimensions of colliding droplets grows, the frequency of the effects of collisions with fragmentation exceeds the corresponding parameter for spreading. At first glance, this result is not quite obvious. However, in analyzing the experiments, we see good reproducibility of the results. Most likely, the revealed effect is due to the fact that, at a multiple excess of the momentum of one droplet over the momentum of the other, their fragmentation takes less energy: the inertial forces are high. As the values of u_m and r_m become closer, for colliding droplets the momentum difference is sufficient for spreading into the same (comparable) droplets.

In the conducted experiments, in analyzing the obtained videograms (analogously to the experiments in [17, 18]) we have recognized three regimes of droplet coagulation (Fig. 8): droplets moving in the wake catch up with those moving ahead of them; droplets reverse the direction of their motion (due to the work of the resistance forces of the gas flow) and coagulate with those in the wake of them; droplets, due to the implementation of phase transformations, coagulate with those moving in parallel at some distance from them (because of the decrease in the static pressure between droplets moving in parallel, the latter move closer together on evaporation). Here, good agreement has also been obtained for the droplets upon coagulation as far as the Weber and Reynolds numbers are concerned. For example, it has been established that, at $0.5 < u_{m1} < 12.5$ m/s, $0.5 < u_{m2} < 4.5$ m/s and $0.075 < r_{m1} < 0.25$, $0.025 < r_{m2} < 0125$ mm, the values of the Weber and Reynolds numbers for combined droplets do not exceed We = 0.25 and Re = 200 respectively. At maximum values of the velocities of motion of the droplets and a significant difference of their dimensions before collision, the Weber and Reynolds numbers for combined droplets are as large as We = 0.3 and Re = 250.

The singled-out features of the coagulation and fragmentation of droplets are in good agreement with the basic propositions of the modern theory of heat and mass transfer and hydrodynamics in gas–droplet systems [34] (in particular, as

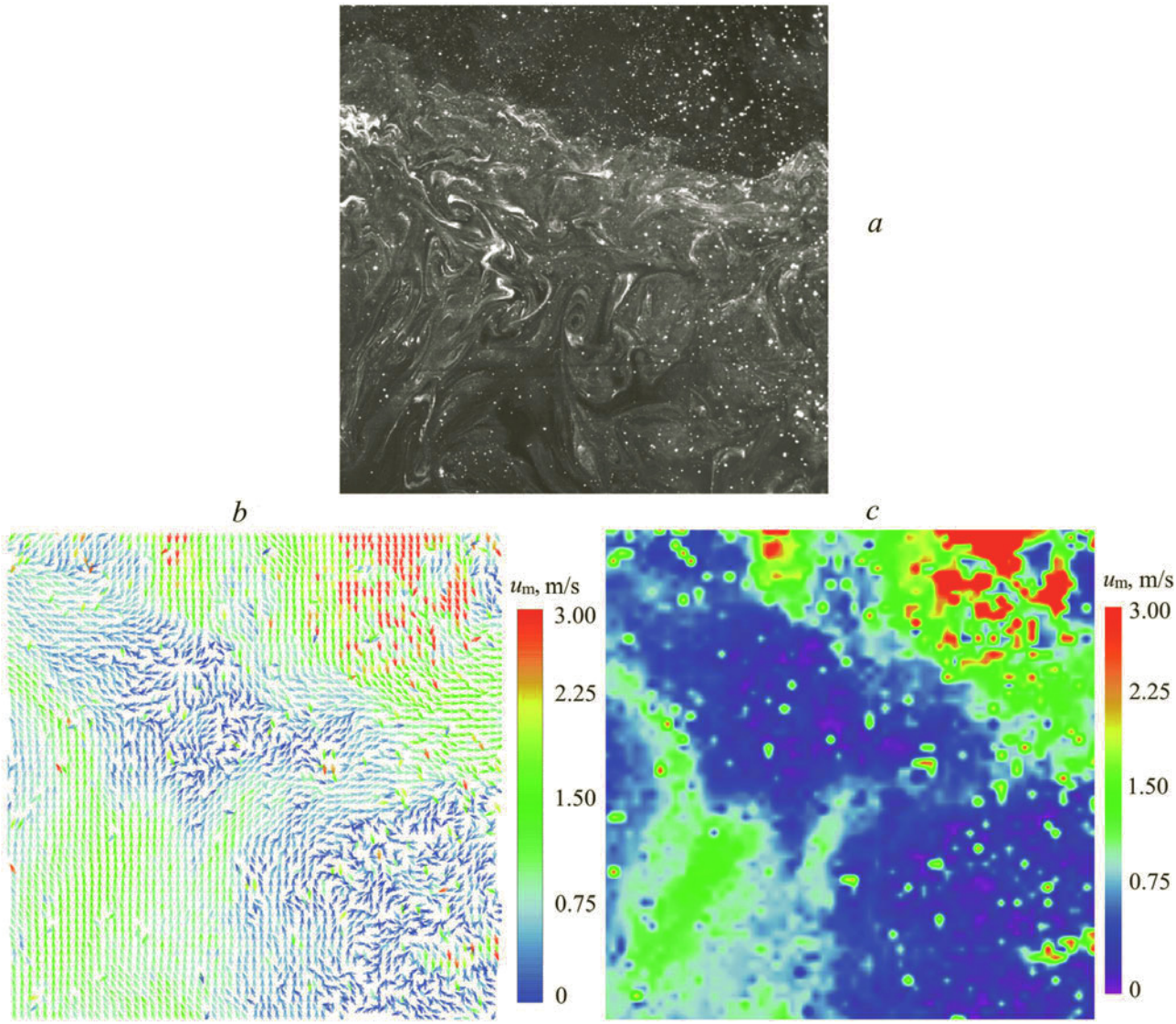

Fig. 5. Videogram of droplets of sprayed water in the flow of high-temperature gases (a) and examples of velocity fields, obtained using "TecPlot" (b) and "ActualFlow" (c) software.

far as the characteristic values of the Weber numbers for droplets are concerned at which we have fragmentation or spreading) and develop the ideas of the experiments of [35–37].

The established features of droplet fragmentation supplement today′s ideas of the features of droplet motion in high-temperature gas flows. In accordance with the results of an analysis of experimental data, we can formulate prognostic models for development of theoretical models of motion of droplets of typical liquids in a flow of high-temperature gases [10–12].

A statistical analysis of results of the performed investigations illustrates the possibility of creating a prognostic apparatus to update the existing gas–vapor–droplet technologies and to develop new technologies for a large group of industries. Among them are mainly [38–45] polydisperse droplet water fire suppression, thermal (evaporative) cleaning of liquids in the gas flow, defrosting of loose media by gas–liquid mixtures, treatment of slagged heat-loaded surfaces of power equipment, droplet condensation in power installations, droplet systems for burning of liquid fuels, and sprinkling gas–liquid systems for special purposes.

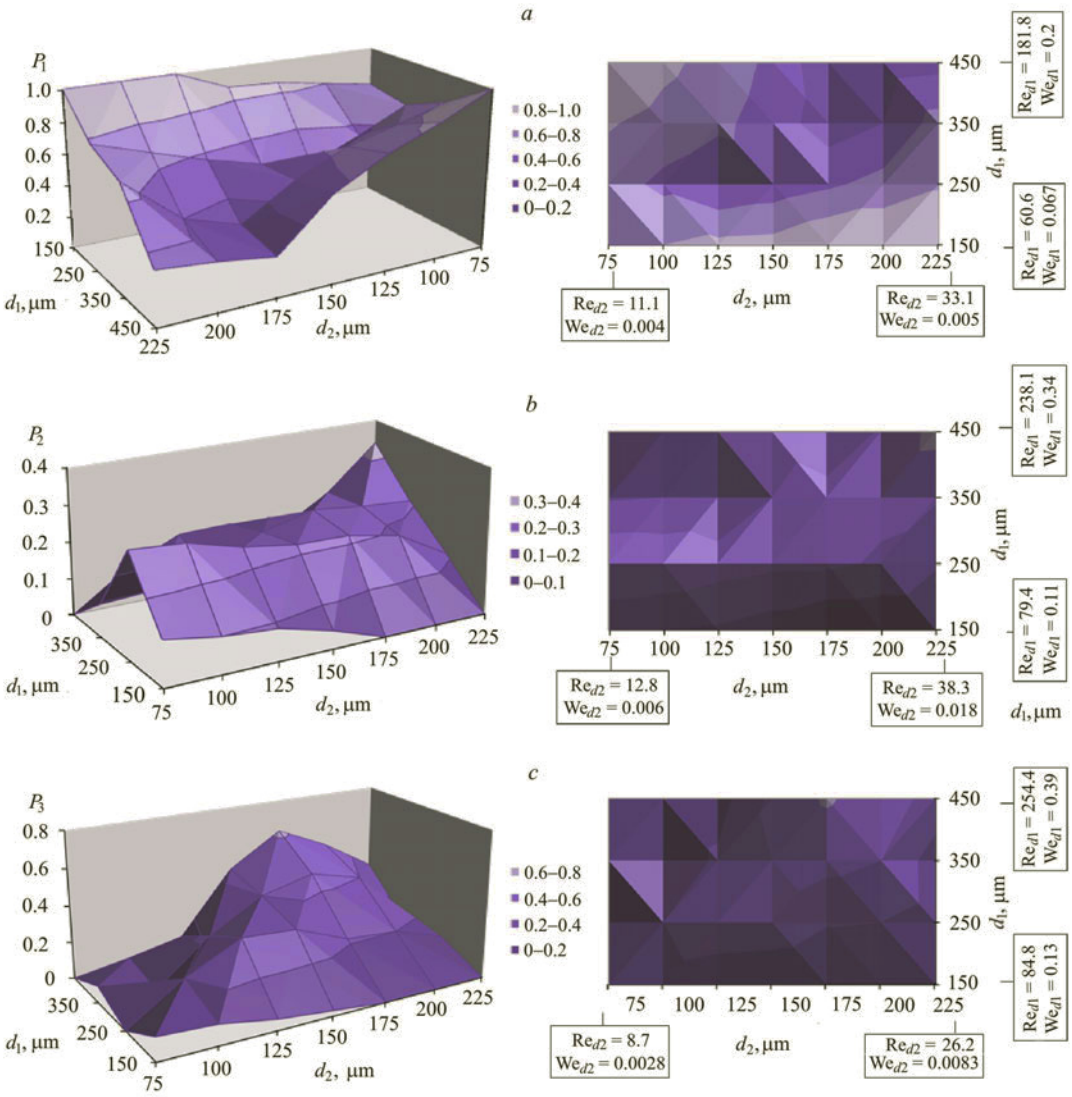

Fig. 6. Statistics of the occurrence of each of the established effects of collision of droplets with variation in the droplet dimensions: a) coagulation, b) spreading, and c) fragmentation.

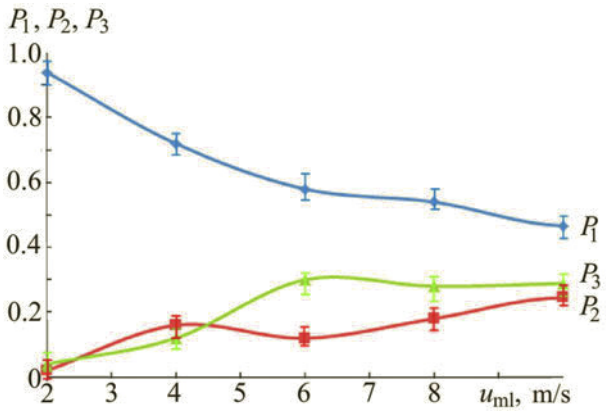

Fig. 7. Statistics of the occurrence of each of the established effects of collision of droplets with variation in the velocities of their motion (at $2 \le u_{m2} \le 3$ m/s, $0.075 < r_{m1} < 0.25$ mm, and $0.025 < r_{m2} < 0.125$ mm): P_1) coagulation, P_2) spreading, and P_3) fragmentation.

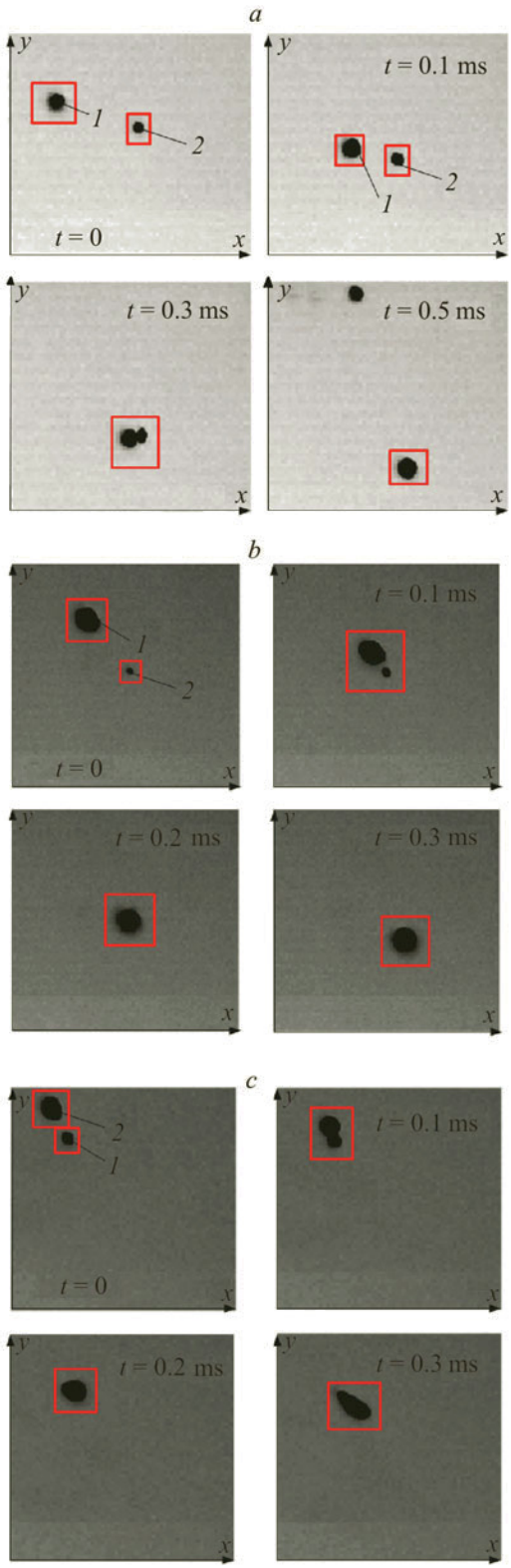

Fig. 8. Typical video frames in the case of implementation of the established coagulation regimes: droplets moving in the wake catch up with those moving ahead (a); droplets reverse the direction of their motion due to the forces of resistance of the gas flow and coagulate with those moving successively (b); droplets, due to the implementation of phase transformations, coagulate with the droplets moving at some distance from them (c).

Conclusions. From the analysis of videograms of the conducted experiments, we have established several typical regimes of collisions of water droplets in a flow of high-temperature gases as a result of which there can occur their coagulation and fragmentation to preserve the initial dimensions (spreading) and to form a large group of droplets of much smaller dimensions. We have determined the initial dimensions and the velocities of motion of the droplets, and also the angles of intersection of their mechanical trajectories at which the revealed regimes are implemented. We have established the characteristic velocities and dimensions of water droplets after coagulation. The revealed regularities make it possible to predict the regimes of droplet collisions under the considered conditions of intense transformations for a large group of applications (e.g., polydisperse vapor–water fire suppression, high-temperature or thermal water purification on power objects, defrosting of loose media by gas–vapor–liquid flows, and cleaning of slagged surfaces of power equipment by gas–vapor–droplet mixtures).

This work was carried out with financial support from a grant of the Russian Science Foundation (project No. 14-39-00003).

NOTATION

d_0, initial dimension of a droplet, mm; P, frequency of implementation of each of the three established variants of effects of collisions; r_m, radius of a droplet, mm; Re, Reynolds number; Re_m, maximum Reynolds number for a droplet; T_g, gas temperature, K; T_w, initial temperature of water droplets introduced into the gas medium, K; u_0, initial velocity of a droplet, m/s; u_g, velocity of motion of the flow of high-temperature gases, m/s; u_m, velocity of motion of droplets, m/s; We, Weber number; We_m, maximum Weber number for a droplet; α_m, angles of intersection of mechanical trajectories of droplets at the instant of their collision, rad; γ_m, volume concentration of droplets; σ, surface tension of the liquid, N/m; ρ_g, gas density, kg/m^3; ν_g, kinematic viscosity of the gas medium, m^2/s.

REFERENCES

1. A. I. Karpov, V. B. Novozhilov, A. A. Galat, and V. K. Bulgakov, Numerical modeling of the effect of fine water mist on the small scale flame spreading over solid combustibles, *Proc. Eighth Int. Symp. "Fire Safety Science,"* **27**, 753–764 (2005).
2. A. Abbud-Madrid, D. Watson, and J. T. McKinnon, On the effectiveness of carbon dioxide, nitrogen and water mist for the suppression and extinction of spacecraft fires, *Suppression and Detection Research and Applications Conference*, Orlando, USA (2007).
3. X. K. Xiao, B. H. Cong, X. S. Wang, K. Q. Kuang, K. K. Yuen Richard, and G. X. Liao, On the behavior of flame expansion in pool fire extinguishment with steam jet, *J. Fire Sci*., **29**, No. 4, 339–360 (2011).
4. T. Carriere, J. R. Butz, S. Naha, A. Brewer, and A. Abbud-Madrid, Fire suppression test using a handheld water mist extinguisher designed for the international space station, *42nd Int. Conf. on Environmental Systems*, California, USA (2012).
5. B. Yao and B. H. Cong, Experimental study of suppressing Poly(methyl methacrylate) fires using water mists, *Fire Safety J*., **47**, 32–39 (2012).
6. Lyndon Macindoe and Justin Leonard, Moisture content in timber decking exposed to bushfire weather conditions, *Fire Mater*., **36**, No. 1, 49–61 (2012).
7. Xiangyang Zhou, Stephen P. D′Aniello, and Hong-Zeng Yu, Spray characterization measurements of a pendent fire sprinkler, *Fire Safety J.*, **54**, 36–48 (2012).
8. B. Rodriquez and G. Young, Development of international space station fine water mist portable fire extinguisher, *43rd Int. Conf. on Environmental Systems*, July 15–18, 2013, Vail, Colorado, USA.
9. R. S. Volkov, G. V. Kuznetsov, and P. A. Strizhak, Numerical assessment of optimum dimensions of droplets of water under the conditions of its spraying by fire-extinguishing facilities in rooms, *Pozharovzryvobezopasnost'*, **21**, No. 5, 74–78 (2012).
10. O. V. Vysokomornaya, G. V. Kuznetsov, and P. A. Strizhak, Heat and mass transfer in the process of movement of water drops in a high-temperature gas medium, *J. Eng. Phys. Thermophys*., **86**, No. 1, 62–68 (2013).
11. P. A. Strizhak, Influence of droplet distribution in a "water slug" on the temperature and concentration of combustion products in its wake, *J. Eng. Phys. Thermophys*., **86**, No. 4, 895–904 (2013).

12. G. V. Kuznetsov and P. A. Strizhak, Numerical investigation of the influence of convection in a mixture of combustion products on the integral characteristics of the evaporation of a finely atomized water drop, *J. Eng. Phys. Thermophys*., **87**, No. 1, 103–111 (2014).
13. R. S. Volkov, O. V. Vysokomornaya, G. V. Kuznetsov, and P. A. Strizhak, Experimental study of the change in the mass of water droplets in their motion through high-temperature combustion products, *J. Eng. Phys. Thermophys*., **86**, No. 6, 1413–1418 (2013).
14. G. V. Kuznetsov and P. A. Strizhak, The motion of a manifold of finely dispersed liquid droplets in the counter flow of high temperature gases, *Tech. Phys. Lett*., **40**, No. 6, 499–502 (2014).
15. G. V. Kuznetsov and P. A. Strizhak, Evaporation of single droplets and dispersed liquid flow in motion through high temperature combustion products, *High Temp*., **52**, No. 4, 568–575 (2014).
16. R. S. Volkov, G. V. Kuznetsov, and P. A. Strizhak, Influence of the initial parameters of spray water on its motion through a counter flow of high temperature gases, *Tech. Phys*., **59**, No. 7, 959–967 (2014).
17. R. S. Volkov, G. V. Kuznetsov, and P. A. Strizhak, Evaporation of two liquid droplets moving sequentially through high-temperature combustion products, *Thermophys. Aeromech.*, **21**, No. 2, 255–258 (2014).
18. R. S. Volkov, G. V. Kuznetsov, and P. A. Strizhak, The influence of initial sizes and velocities of water droplets on transfer characteristics at high-temperature gas flow, *Int. J. Heat Mass Transf.*, **79**, 838–845 (2014).
19. J. Westerweel, Fundamentals of digital particle image velocimetry, *Meas. Sci. Technol.*, **8**, 1379–1392 (1997).
20. J. M. Foucaut and M. Stanislas, Some considerations on the accuracy and frequency response of some derivative filters applied to particle image velocimetry vector fields, *Meas. Sci. Technol.*, **13**, 1058–1071 (2002).
21. J. V. Simo-Tala, S. Russeil, D. Bougeard, and J.-L. Harion, Investigation of the flow characteristics in a multirow finned-tube heat exchanger model by means of PIV measurements, *Exp. Therm. Fluid Sci.*, **50**, 45–53 (2013).
22. C. Willert, Assessment of camera models for use in planar velocimetry calibration, *Exp. Fluids*, **41**, No. 1, 135–143 (2006).
23. N. Damaschke, H. Nobach, and C. Tropea, Optical limits of particle concentration for multi-dimensional particle sizing techniques in fluid mechanics, *Exp. Fluids*, **32**, No. 2, 143–152 (2002).
24. E. K. Akhmetbekov, D. M. Markovich, and M. P. Tokarev, Correlation correction in the method of tracking of particles in flows, *Vych. Tekhnol*., **15**, No. 4, 57–72 (2010).
25. E. A. Ibrahim, H. Q. Yangt, and A. J. Przekwas, Modeling of spray droplets deformation and breakup, *J. Propuls. Power*, **9**, No. 4, 651–654 (1993).
26. S. S. Hwang, Z. Liu, and R. D. Reitz, Breakup mechanisms and drag coefficients of high-speed vaporizing liquid drops, *Atomization Sprays*, **6**, No. 3, 353–376 (1996).
27. A. A. Shreiber, A. M. Podvisotski, and V. V. Dubrovski, Deformation and breakup of drops by aerodynamic loads, *Atomization Sprays*, **6**, No. 6, 667–692 (1996).
28. J. Eggers and E. Villermaux, Physics of liquid jets, *Rep. Prog. Phys.*, **71**, No. 036601, 1–79 (2008).
29. A. K. Flock, D. R. Guildenbecher, J. Chen, P. E. Sojka, and H. J. Bauer, Experimental statistics of droplet trajectory and air flow during aerodynamic fragmentation of liquid drops, *Int. J. Multiphase Flow*, **47**, 37–49 (2012).
30. J. E. Sprittles and Y. D. Shikhmurzaev, Coalescence of liquid drops: Different models versus experiment, *Phys. Fluids*, **24**, No. 122105, 1–27 (2012).
31. H. Shank, *Theory of Engineering Experiments* [Russian translation], Mir, Moscow (1972).
32. A. N. Zaidel, *Elementary Estimates of Measurement Errors* [in Russian], 3rd revised and supplemented edn., Nauka, Leningrad (1968).
33. Yu. V. Polezhaev and F. B. Yurevich, *Thermal Protection* [in Russian], Énergiya, Moscow (1976).
34. V. I. Terekhov and M. A. Pakhomov, *Heat and Mass Transfer and Hydrodynamics in Gas–Droplet Flows* [in Russian], Izd. NGTU, Novosibirsk (2009).
35. A. G. Girin, Equations of the kinetics of droplet fragmentation in a high-speed gas flow, *J. Eng. Phys. Thermophys*., **84**, Issue 2, 262–269 (2011).
36. A. G. Girin, Distribution of dispersed droplets in fragmentation of the drop in a high-velocity gas flow, *J. Eng. Phys. Thermophys*., **84**, Issue 4, 805–812 (2011).
37. A. G. Girin, Laws governing the fragmentation of a droplet in a high-speed stream, *J. Eng. Phys. Thermophys*., **84**, Issue 5, 1009–1015 (2011).
38. M. N. Nikitin, Influence of directed water injection in the heat generator on the pressure of the produced vapor–gas mixture, *Prom. Énerg.*, No. 6, 42–46 (2010).

39. M. N. Nikitin, Use of a vapor–gas mixture in fuel burning, *Prom. Énerg.*, No. 12, 37–42 (2010).
40. A. V. Efimov, A. L. Goncharenko, O. V. Kasilov, and L. V. Goncharenko, Selection of the optimum parameters of heat-transfer agents in developing systems for deep utilization of the heat of gases escaping from boiler units, *Énergosber., Énergetika, Énergoaudit*, No. 3 (121), 2–11 (2014).
41. V. F. Pershin, V. G. Odnol′ko, and S. V. Pershina, *Recycling of Loose Materials in Barrel-Type Machines* [in Russian], Mashinostroenie, Moscow (2009).
42. E. A. Isaev, I. E. Chernetskaya, L. N. Krakht, and V. S. Titov, *Theory of Control over the Pelletizing of Loose Materials* [in Russian], TNT, Staryi Oskol (2012).
43. B. N. Mar′in, V. A. Kim, and O. E. Sysoev, *Treatment of Surfaces in Metallurgy and Machine Construction* [in Russian], Dal′nauka, Vladivostok (2011).
44. I. D. Ibatullin, *Kinetics of Fatigue Damageability and Failure of Surface Layers* [in Russian], SGTU, Samara (2008).
45. R. Negeed El-Sayed, M. Albeirutty, and Y. Takata, Dynamic behavior of micrometric single water droplets impacting onto heated surfaces with TiO_2 hydrophilic coating, *Int. J. Therm. Sci.*, **79**, 1–17 (2014).